31st Annual International Conference of the IEEE EMBS
Minneapolis, Minnesota, USA, September 2-6, 2009

Realization of a 15-Channel, Hermetically-Encased Wireless Subretinal Prosthesis for the Blind

Shawn K. Kelly, Member, IEEE, Douglas B. Shire, Member, IEEE, Jinghua Chen, Patrick Doyle, Marcus D. Gingerich, William A. Drohan, Member, IEEE, Luke S. Theogarajan, Stuart F. Cogan, Member, IEEE, John L. Wyatt, Senior Member, IEEE, and Joseph F. Rizzo, III.

***Abstract*—A miniaturized, hermetically-encased, wirelessly-operated retinal prosthesis has been developed for implantation and pre-clinical studies in Yucatan mini-pig animal models. The prosthesis conforms to the eye and drives a microfabricated polyimide stimulating electrode array with sputtered iridium oxide electrodes. This array is implanted in the subretinal space using a specially-designed *ab externo* surgical technique that affixes the bulk of the prosthesis to the surface of the sclera. The implanted device includes a hermetic titanium case containing a 15-channel stimulator chip and discrete power supply components. Feedthroughs from the case connect to secondary power- and data-receiving coils. In addition, long-term *in vitro* pulse testing was performed on the electrodes to ensure their stability for the long lifetime of the hermetic case. The final assembly was tested *in vitro* to verify wireless operation of the system in biological saline using a custom RF transmitter circuit and primary coils. Stimulation pulse strength, duration and frequency were programmed wirelessly using a custom graphical user interface. Operation of the retinal implant has been verified *in vivo* in one pig for more than three months by measuring stimulus artifacts on the eye surface using a contact lens electrode.**

I. Introduction

RETINAL prostheses are actively being developed by a number of groups worldwide [1]–[12]. These devices aim to restore visual function lost due to degenerative retinal diseases such as retinitis pigmentosa (RP) and age-related macular degeneration (AMD). These conditions cause a gradual loss of photoreceptors, yet a substantial fraction of the retinal ganglion cells remain, forming intact neural pathways from the retina to the visual cortex. The prevalence of RP is approximately 1 in every 4000 live births, and there are approximately 1,700,000 affected individuals worldwide. AMD is the leading cause of blindness in the developed world, with roughly 2 million affected patients in the United States alone. This number is expected to increase by 50% by the year 2020 as the population ages [13]. The best existing treatments slow the progress of these diseases, but no cure is known. While it is evident that significant reorganization of the retina occurs after the loss of input signals from the photoreceptors [14], our group and others have nevertheless demonstrated that focal electrical stimulation of the retinal ganglion cells can yield responses that correspond to the strength and location of the stimuli (e.g., [15]). However, while our group's acute stimulation trials in humans produced visual percepts, they were not as detailed as we had hoped [2], [3]. It became evident to our team after these studies that a chronically implantable device was required to fully explore the prospects of restoring useful vision.

Other groups are also actively engaged in similar efforts (e.g., [8]–[12]). The majority of the groups working in visual prosthetics today are concentrating either on direct epiretinal [4], [5] or subretinal [6], [7] electrical stimulation, or on less direct stimulation of the retina using a supra-choroidal or trans-scleral approach [8]–[10]. For a number of years, our team's approach focused on epiretinal prosthesis design, culminating in several acute human surgical trials using flexible, polyimide-based stimulating electrode arrays comparable to those in our present design [2], [3]. A number of factors, however, eventually led our group to take an ab externo, subretinal surgical approach to chronic implantation of a wirelessly driven microstimulator. This design approach yields improved biocompatibility and a less-invasive surgery, and it leaves the bulk of the implant device outside the eye.

Our first-generation wirelessly-powered implantable retinal stimulation device [1] was implanted in Yucatan mini-pigs during the spring and summer of 2008. We now describe an improved version of the implant, with the circuits encased in a hermetic titanium enclosure, the coils moved to a more magnetically-favorable position, and easier

Manuscript received April 24, 2009. This work was supported in part by the VA Center for Innovative Visual Rehabilitation, NIH (EY016674-01), NSF (IIS-0515134), the Catalyst Foundation, and the MOSIS Service.

S. K. Kelly is with the VA Boston Healthcare System (VABHS) and the Massachusetts Institute of Technology (MIT), Cambridge, MA 02139 USA (phone: 617-324-1890; fax: 617-258-5846; e-mail: skkelly@alum.mit.edu).

D. B. Shire is with the VABHS and Cornell University, Ithaca, NY 14853 USA (e-mail: dbs6@cornell.edu).

J. Chen is with the Massachusetts Eye and Ear Infirmary (MEEI), Boston, MA 02114 USA (e-mail: jinghua_chen@meei.harvard.edu).

P. Doyle is with the Boston VA Research Institute and MIT, Cambridge, MA 02139 USA (e-mail: wpd@mit.edu).

M. D. Gingerich is with the VABHS and Cornell University, Ithaca, NY 14853 USA (e-mail: mdg37@cornell.edu).

W. A. Drohan is with the VABHS and MIT, Cambridge, MA 02139 USA (e-mail: billd@mit.edu).

L. S. Theogarajan is with University of California, Santa Barbara, CA 93106 USA (e-mail: ltheogar@ece.ucsb.edu).

S. F. Cogan is with EIC Laboratories, Inc. Norwood, MA 02062 USA (e-mail: scogan@eiclabs.com).

J. L. Wyatt is with MIT, Cambridge, MA 02139 USA (e-mail: jlw@mit.edu).

J. F. Rizzo, III, is with the VABHS and MEEI, Boston, MA 02114 USA (e-mail: joseph_rizzo@meei.harvard.edu).

surgical access for electrode array insertion. We have also performed significantly more testing of our thin-film microfabricated electrode array.

II. Retinal Implant Design and Methods

A. System Description

Our implant system consists of a computer-based controller with a user interface for selecting which electrodes to drive, and with which level of current. Data from the computer system are sent to a power amplifier, which then transmits wirelessly to the implant by near-field inductive coupling. Data at 100 Kbps are encoded by amplitude shift keying on a 15.5 MHz carrier. Power is also wirelessly transmitted to the implant using a 125 KHz carrier, and is rectified by the implant to create ±2.5 V power supplies.

The implant itself is attached to the outside of the eye, where it receives and processes the power and data. The implant then sends electrical stimulation current to the retinal nerve cells via a thin-film microfabricated array of sputtered iridium oxide film (SIROF) electrodes, which is surgically inserted into the subretinal space through a flap in the sclera.

B. Differences from First-Generation Device

Our first-generation device [1] was assembled on a flexible substrate that wrapped around the eye, attaching to the sclera of the eye, inside the socket (Fig. 1). This device had three significant design drawbacks: (1) small receiver coils made power and data telemetry difficult; (2) the silicone coating held up well in studies of a few months, but would not be viable for chronic trials of many years; and (3) the required surgical approach for electrode array insertion is very difficult, since the coils are in the way. In addition, we had relatively little data about the long-term survivability of our electrode arrays under continuous stimulation.

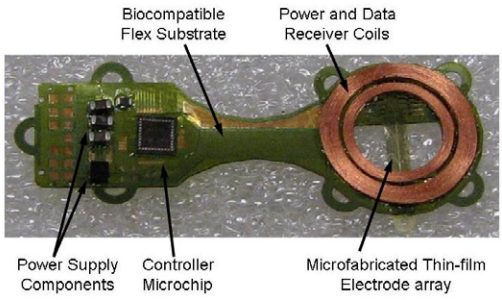

Fig. 1. First-generation retinal prosthesis. This flexible device wraps around the eye, with the coils in the superior-temporal quadrant, and the controller circuitry in the superior-nasal quadrant. The electrode array inserts through a flap in the sclera to access the subretinal space. Primary power and data coils rest on the face, on the temporal side.

Our newer-generation device uses the same controller chip [16] and power and data telemetry scheme, but solves the three problems outlined above, with, respectively: (1) larger coils, conforming to the eye, surrounding the cornea, under the conjunctiva; (2) a hermetic, titanium case enclosing the circuitry, attached to the sclera deep in the superior-nasal quadrant; and (3) a serpentine electrode array which extends from the case to the superior-temporal quadrant, giving open surgical access to create the scleral flap and insert the array into the subretinal space. The concept of this hermetic implant is shown in Fig. 2.

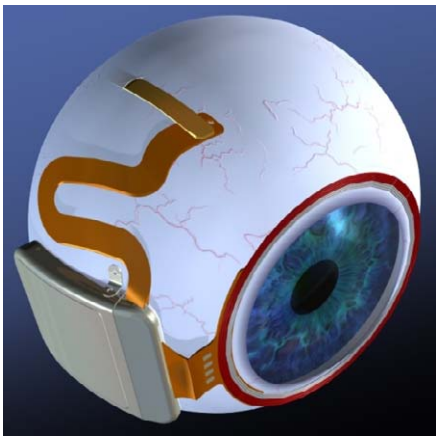

Fig. 2. Drawing of hermetic implant concept. The power and data receiver coils are now on the front of the eye, just behind the conjunctiva. The electronics are enclosed in a hermetic titanium case, and the electrode array insertion is in its own quadrant for ease of surgical access.

C. Improved Implant Components

Relocating the secondary power and data coils from the temporal side of the eye to the anterior of the eye allowed for much larger coils, giving much better inductive coupling. However, these coils rest against the delicate conjunctiva and can wear through, creating a risk of infection. To reduce this risk, the coils are carefully wound on a sphere so that they match the curvature of the eye. The secondary coils include both power and data, but they are wound together for structural support. They are made of 40 AWG gold wire, with 28 turns for the power coil and two 6-turn coils for a 12-turn center-tapped data receiver. The spherically-molded coil has a mean radius of 9.5 mm and a height off of the eye of less than 0.2 mm. The secondary coils are shown on a model eye in Fig. 3.

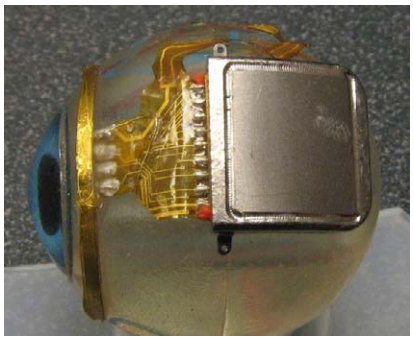

Fig. 3. Hermetic retinal prosthesis, a prototype of the device in Fig. 2. The gold power and data secondary coils are wound on a sphere to match the eye curvature. The machined titanium case with welded lid has a hermetic ceramic feedthrough. The serpentine electrode array is out of view over the top of the model eye.

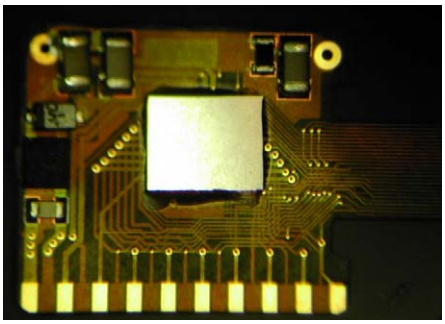

Fig. 4. Retinal implant circuit board. The controller IC, along with power supply and signal conditioning components, is inserted into the curved hermetic titanium case.

The integrated circuit, which includes the telemetry receiver, digital controller, analog current sources, biases, and startup circuitry, is encased in the curved titanium enclosure measuring 11 mm x 11 mm x 2 mm. Additionally, Schottky rectifier diodes, two power supply capacitors, a discrete resistor and capacitor for power-up reset delay, a resonating capacitor for the power secondary coil, and a 5.1 V Zener diode for power supply regulation are included in the package. The circuit board included in the hermetic package is shown in Fig. 4.

The novel, serpentine design of our flexible, thin-film electrode array allows the surgeon to route it behind the superior rectus muscle and insert the electrodes into the superior-temporal quadrant. Since the titanium case is in the superior-nasal quadrant and the secondary coil is low-profile, there is nothing blocking surgical access to the scleral flap.

D. Long-term Electrode Pulsing

Encasing the electronics in titanium allows this device to be implanted for a much longer time than the first-generation device. This longer-term implantation requires additional testing of the microfabricated SIROF electrodes under chronic pulsing. To assess their stability for chronic animal implantation, we subjected the SIROF electrodes to long-term *in vitro* pulsing. Arrays with sixteen 400 μm diameter electrodes were pulsed at 37°C in an inorganic model of interstitial fluid [17]. The multichannel stimulators for the *in vitro* pulsing employ circuits generating an electrical current pulse protocol similar to those used in the implant for animal testing. Eight electrodes on each array were pulsed at a charge density of 200 μC/cm^2 (1 ms pulse width, 50 Hz repetition rate) using a 0.6 V Ag/AgCl interpulse bias [18].

E. Implant Testing

The full implant system was tested dry on the bench, as well as *in vitro* in a phosphate buffered saline solution. Electrodes were driven with balanced biphasic pulses of current, 25-200 μA, with the duration of each phase being 1 ms. Similar stimulation parameters were used during *in vivo* stimulation trials performed in the Yucatan mini-pig.

During wireless *in vitro* tests, no test points were available, so needle electrodes were immersed in the saline, and the differential voltage was measured with a custom-built instrumentation amplifier. The same type of measurement was made *in vivo* with a contact lens electrode on the eye surface and an ear reference electrode to ensure that the device was working in the pig eye. These measurements were entirely non-invasive.

III. RESULTS

A. Long-term Electrode Pulsing

An example of the voltage transients from eight electrodes on one array and a representative current waveform are shown in Fig. 5. The voltage transients are quite similar for the eight electrodes with maximum cathodal potential (Emc) of about 0.4 V Ag|AgCl, well positive of the –0.6 V water reduction potential on SIROF. Cyclic voltammetry in the model-ISF also showed a consistency in electrode response and good stability over long-term pulsing. In Fig. 6, the voltammograms of the eight pulsed electrodes are compared after 670 hr and 2900 hr of pulsing. The origin of the observed changes in the CV response between 670 hr and 2900 hr is uncertain, although the observed changes are consistent with a decrease in the density of the SIROF due to hydration.

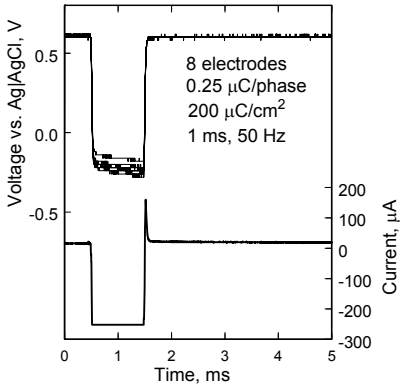

Fig. 5. Voltage transients of eight SIROF electrodes on a polyimide array. The electrodes have been pulsed for 2900 hr at 200 μC/cm^2. A representative current waveform is also shown.

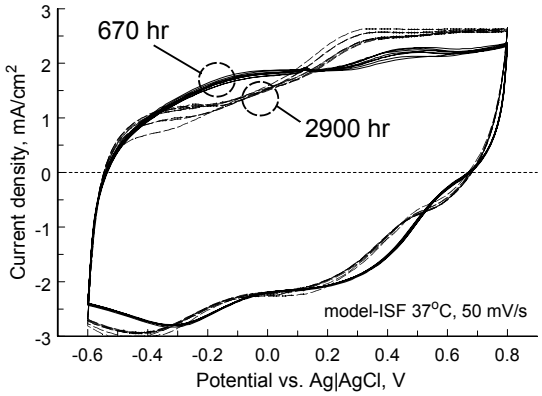

Fig. 6. Cyclic voltammograms of eight SIROF electrodes after 670 hr (solid) and 2900 hr (dashed) of pulsing at 200 μC/cm^2.

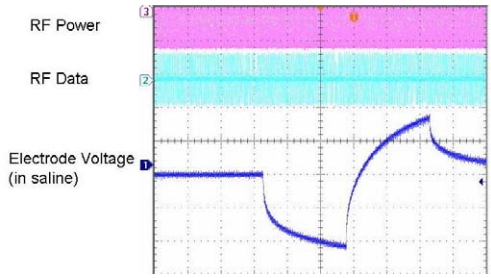

Fig. 7. Electrode test waveform for a wirelessly-driven implant. The bottom waveform shows the electrode voltage in saline, measured via a test tail which is trimmed off before surgery.

B. *Implant in Vitro and in Vivo Testing*

A typical electrode test waveform is shown in Fig. 7. This type of waveform shows not only the resistive portions of the fluid and the electrode access resistance, but also the charging of the electrode-tissue interface. Examples from stimulation of the mini-pig eye are shown in Fig. 8. Because of the measurement setup, these waveforms show only the resistive voltage of current flowing through fluid. The waveforms show a great deal of variance, largely due to inconsistencies in the placement of the contact lens electrode and the use of a distant reference electrode on the ear. However, this measurement method was non-invasive, and it greatly simplified the testing, allowing for non-sterile follow-up studies after surgical implantation of the device.

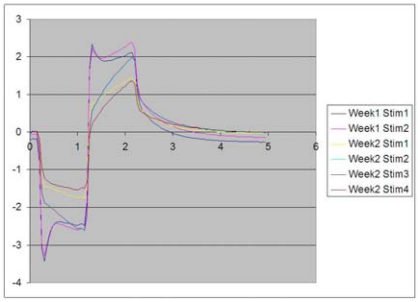

Fig. 8. Measured electrical stimulus artifact from the mini-pig eye. The wide variation in waveform size and shape has mostly to do with the variation in placement of the contact lens electrode on the eye.

IV. Conclusion

The hermetic retinal prosthesis device presented here is capable of being implanted for a much longer time than our previous silicone-coated device. This allows for the 10-year survivability expected by the FDA for clinical trials. Our implant worked reliably during animal testing for over three months, though exposure problems at the conjunctiva forced an early end to the experiment. We have slightly redesigned the coil molding process and the connection between the case and the coil to ease the tension on the conjunctiva for future trials. These modifications will allow longer-term animal implantation trials in the near future, with a view toward human clinical trials, and the ultimate goal of a subretinal prosthesis capable of restoring useful vision to blind patients.

References

[1] D. B. Shire, S. K. Kelly, J. Chen, P. Doyle, M. D. Gingerich, S. F. Cogan, W. Drohan, O. Mendoza, L. Theogarajan, J. L. Wyatt, J. F. Rizzo, "Development and Implantation of a Minimally-Invasive, Wireless Sub-Retinal Neurostimulator," *IEEE Trans. Biomed. Eng*., accepted for publication in March, 2009.

[2] J. F. Rizzo III, J. Wyatt, J. Loewenstein, S. Kelly, and D. Shire, "Perceptual Efficacy of Electrical Stimulation of Human Retina with a Microelectrode Array During Short-Term Surgical Trials," *Invest. Ophthalmol. Vis. Sci.*, vol. 44, pp. 5362-5369, 2003.

[3] J. F. Rizzo III, J. Wyatt, J. Loewenstein, S. Kelly, and D. Shire, "Methods and Perceptual Thresholds for Short-Term Electrical Stimulation of Human Retina with Microelectrode Arrays," *Invest. Ophthalmol. Vis. Sci*., vol. 44, pp. 5355-5361, 2003.

[4] D. Yanai, J. D. Weiland, M. Mahadevappa, R. J. Greenberg, I. Fine, and M. S. Humayun, "Visual Performance Using a Retinal Prosthesis in Three Subjects with Retinitis Pigmentosa," *Am. J. Ophthalmol*., vol. 143, pp. 820-827, 2007.

[5] H. Gerding, F. P. Benner, and S. Taneri, "Experimental Implantation of Epiretinal Retina Implants (EPI-RET) With an IOL-Type Receiver Unit," *J. Neural Eng*., vol. 4, pp. S38-S49, 2007.

[6] P. J. DeMarco, Jr., G. L. Yarbrough, C. W. Yee, G. Y. Mclean, B. T. Sagdullaev, S. L. Ball, and M. A. McCall, "Stimulation via a Subretinally Placed Prosthetic Elicits Central Activity and Induces a Trophic Effect on Visual Responses," *Invest. Ophthalmol. Vis. Sci*., vol. 48, pp. 916-926, 2007.

[7] T. Schanze, H. G. Sachs, C. Wiesenack, U. Brunner, and H. Sailer, "Implantation and Testing of Subretinal Film Electrodes in Domestic Pigs," *Exp. Eye Res*., vol. 82, pp. 332-340, 2006.

[8] J. A. Zhou, S. J. Woo, S. I. Park, E. T. Kim, J. M. Seo, H. Chung, and S. J. Kim, "A Suprachoroidal Electrical Retinal Stimulator Design for Long-Term Animal Experiments and In-Vivo Assessment of Its Feasibility and Biocompatibility in Rabbits," *J. Biomed. Biotech*., vol. 2008, Article ID 547428, 10 pp., 2008.

[9] Y. T. Wong, N. Dommel, P. Preston, L. E. Hallum, T. Lehmann, N. H. Lovell, and G. J. Suaning, "Retinal Neurostimulator for a Multifocal Vision Prosthesis," *IEEE Trans. Neural Syst. Rehab. Eng*., vol. 15, pp. 425-434, 2007.

[10] Y. Terasawa, H. Tashiro, A. Uehara, T. Saitoh, M. Ozawa, T. Tokuda, and J. Ohta, "The Development of a Multichannel Electrode Array for Retinal Prostheses," *J. Artif. Organs*, vol. 9, pp. 263-266, 2006.

[11] R. Hornig, T. Zehnder, M. Velikay-Parel, T. Laube, M. Feucht, and G. Richard, "The IMI Retinal Implant System," in M. S. Humayun, J. D. Weiland, G. Chader, and E. Greenbaum, eds., *Artificial Sight: Basic Research, Biomedical Engineering, and Clinical Advances*, New York: Springer, pp. 111-128, 2007.

[12] E. Zrenner, "Restoring Neuroretinal Function: New Potentials," *Doc. Ophthalmol*., vol. 115, pp. 56-59, 2007.

[13] D. Friedman, B. O'Colmain, B. Muñoz, S. C. Tomany, C. McCarty, P. T. de Jong, B. Nemesure, P. Mitchell, and J. Kempen, "Prevalence of Age-Related Macular Degeneration in the United States," *Arch. Ophthalmol*., vol. 122, pp. 564-572, 2004.

[14] R. E. Marc, B. W. Jones, J. R. Anderson, K. Kinard, D. W. Marshak, J. H. Wilson, T. G. Wensel, and R. J. Lucas, "Neural Reprogramming in Retinal Degenerations," *Invest. Ophthalmol. Vis. Sci*., vol. 48, pp. 3364-3371, 2007.

[15] R. J. Jensen and J. F. Rizzo III, "Responses of Ganglion Cells to Repetitive Electrical Stimulation of the Retina," *J. Neural Eng*., vol. 4, pp. S1-S6, 2007.

[16] L. S. Theogarajan, "A Low-Power Fully Implantable 15-Channel Retinal Stimulator Chip," *IEEE J. Solid-State Circuits*, vol. 43, pp. 2322-2337, 2008.

[17] S. F. Cogan, P. R. Troyk, J. Ehrlich, C. M. Gasbarro, and T. D. Plante, "The Influence of Electrolyte Composition on the In Vitro Charge-Injection Limits of Activated Iridium Oxide (AIROF) Stimulation Electrodes," *J. Neural Eng.,* vol. 4, pp. 79-86, 2007.

[18] S. F. Cogan, P. R. Troyk, J. Ehrlich, and T. D. Plante, "In Vitro Comparison of the Charge-Injection Limits of Activated Iridium Oxide (AIROF) and Platinum-Iridium Microelectrodes," *IEEE Trans Biomed Eng.*, vol. 52, pp. 1612-1614, 2005.